

Frustrated H-Induced Instability of Mo (110)

Bernd Kohler, Paolo Ruggerone, Steffen Wilke, and Matthias Scheffler

Fritz-Haber-Institut der Max-Planck-Gesellschaft, Faradayweg 4-6, D-14 195 Berlin-Dahlem, Germany

(submitted 25 May 1994)

Using helium atom scattering Hulpke and Lüdecke recently observed a giant phonon anomaly for the hydrogen covered W (110) and Mo (110) surfaces. An explanation which is able to account for this and other experiments is still lacking. Below we present density-functional theory calculations of the atomic and electronic structure of the clean and hydrogen-covered Mo (110) surfaces. For the full adsorbate monolayer the calculations provide evidence for a strong Fermi surface nesting instability. This explains the observed anomalies and resolves the apparent inconsistencies of different experiments.

PACS numbers: 68.35.-p, 73.20.-r, 73.20.Mf

Recently, giant anomalies in the surface phonon spectra have been detected by helium atom scattering (HAS) on the (110) surfaces of tungsten and molybdenum, when these are covered with a full monolayer of hydrogen [1–3]. One critical wave vector $\mathbf{Q}_{c1}^{\text{exp}}$ is along the [001] direction ($\overline{\Gamma\text{H}}$) and has a length of 0.95 \AA^{-1} for W and 0.90 \AA^{-1} for Mo. Anomalies have also been found for directions deviating from $\overline{\Gamma\text{H}}$. Along $\overline{\Gamma\text{S}}$ they are located at $\overline{\text{S}}$ with a critical wave vector $\mathbf{Q}_{c2}^{\text{exp}}$ ($|\mathbf{Q}_{c2}^{\text{exp}}| = 1.225 \text{ \AA}^{-1}$ for Mo and 1.218 \AA^{-1} for W) [4]. The experimental dispersion curves (see Ref. [3]) are only available for $\overline{\Gamma\text{H}}$ and $\overline{\Gamma\text{S}}$. Thus, we focus our attention particularly on these two directions. For both surfaces two different softenings in the surface phonon branches were observed at the critical wave vectors: a smaller dip and a very deep and sharp indentation from $\hbar\omega \approx 15 \text{ meV}$ to $\hbar\omega \approx 2 \text{ meV}$. Only the phonon dispersion curves of quasi-one-dimensional conductors, like KCP [$\text{K}_2\text{Pt}(\text{CN})_4\text{Br}_3$] [5] are characterized by similarly deep anomalies strongly localized in reciprocal space. A pronounced but less sharp damping of longitudinal surface phonons was observed for the (100) surfaces of W [6,7] and Mo [8] and was explained in terms of the nested structure of the Fermi surface [9,10]. In the case of W (100) this Fermi surface nesting is apparently so strong that it induces a rebonding at the surface and a structural rearrangement, i.e. a $c(2 \times 2)$ surface reconstruction at temperatures below $T_c \approx 250 \text{ K}$ (for a review see [11]). For the clean (110) surfaces of W and Mo no indication of an anomaly is found, but this only appears when the surfaces are covered with a full layer of hydrogen. Nevertheless, a close link between the surface phonon anomalies and H vibrations seems to be ruled out, since the HAS spectra remain practically unchanged when deuterium is adsorbed instead of hydrogen [2,3].

Angular resolved photoemission (ARP) studies have been performed by Kevan and coworkers [12–14] for clean and hydrogen covered W (110) and Mo (110). These

studies give no evidence of the existence of parallel segments of the Fermi-surface contours separated by wave vectors comparable with the HAS determined critical wave vectors and thus there appeared to be compelling reason for abandoning the nesting mechanism as a possible origin of the anomalies seen in HAS.

The situation became even more puzzling when very careful high resolution electron energy loss spectroscopy (HREELS) studies [15] of hydrogen covered W (110) observed the Rayleigh wave phonon branch with the small dip at $\mathbf{Q}_{c1}^{\text{exp}}$ exactly as the HAS results. However, the giant anomaly was not detected.

At present there exists no explanation which is able to account for the observed two phonon anomalies and is compatible with the different experimental data (HAS, HREELS, and ARP). We therefore performed *ab-initio* calculations of the surface atomic geometries and the electronic properties of the clean and H-covered Mo (110) surface. The results for the adsorbate covered surface provide clear evidence for a Fermi surface nesting instability at wave vectors which are in remarkable agreement with those at which the phonon anomalies occur for this system [$\mathbf{Q}_{c1}^{\text{th}} = (0.86 \pm 0.02, 0) \text{ \AA}^{-1}$, $\mathbf{Q}_{c1}^{\text{exp}} = (0.90, 0) \text{ \AA}^{-1}$, $\mathbf{Q}_{c2}^{\text{th}} = (1.00 \pm 0.02, 0.71 \pm 0.02) \text{ \AA}^{-1}$, $\mathbf{Q}_{c2}^{\text{exp}} = (1.00, 0.707) \text{ \AA}^{-1}$]. We choose the x -axis along [001] and the y -axis is along $\overline{\Gamma\text{H}}$. The corresponding directions in reciprocal space are $\overline{\Gamma\text{H}}$ and $\overline{\Gamma\text{N}}$, respectively. The calculations were performed using density-functional theory together with the local-density approximation for the exchange-correlation energy functional [16]. The full-potential linearized augmented plane wave method [17] is employed which we enhanced by the calculation of forces [18]. This enables an efficient evaluation of the multi-layer substrate relaxation and the atomic positions at the surface. The substrate is modeled by a seven layer slab repeated periodically with a separation of 8.8 \AA of vacuum. The \mathbf{k} -integrations are evaluated on a mesh of 64 equally spaced points in the surface Brillouin zone (SBZ). The muffin-tin radii are chosen to be 1.27 \AA and 0.48 \AA for Mo and H, respectively. The kinetic-energy cutoff for the plane wave basis needed for the interstitial region is set to 12 Ry, and the (l, m) representation (inside the muffin tins) is taken up to $l_{\text{max}} = 8$. For the potential expansion we use a plane-wave cutoff energy of 64 Ry and a (l, m) representation with $l_{\text{max}} = 4$. The core states as well as the valence states are treated non-relativistically. The calculated in-plane lattice constant is 3.13 \AA without including zero point vibrations, which compares well with the measured bulk lattice parameter

(3.148 Å at room temperature [19]). The values of the surface relaxation for the clean surface are in excellent agreement with those calculated by Methfessel *et al.* [20] who employed the full-potential linearized muffin-tin orbitals approach.

For a meaningful theoretical analysis of the surface electronic structure it is important to use the correct atomic geometry. For the hydrogen adsorption system at a full monolayer, i.e. at the coverage for which the phonon anomaly was observed experimentally, neither the hydrogen adsorption site nor the substrate relaxation have been determined so far. In Table I we summarize the calculated adsorption energy differences ΔE_{ad} as well as the relaxation parameters for all possibly important hydrogen sites. The geometries are defined in Fig. 1. The results identify the hollow site as the most stable position. The $[\bar{1}10]$ -offset from the long-bridge position is $y_{\text{H}} = 0.55 \pm 0.01$ Å. Within the computational error the hydrogen relaxes exactly in the geometric threefold site and there is no theoretical evidence for a pronounced top-layer-shift reconstruction in agreement with the low-energy electron diffraction experiments [21]. In comparison both bridge positions are clearly energetically unfavorable, and the on-top position is even worse. The theory predicts that the clean-surface inward relaxation of -4.5% d_0 , where d_0 is the bulk inter-layer spacing, is reduced for the long-bridge, short-bridge, and hollow geometries of the adsorbed hydrogen. In the case of the on-top adsorption site we obtain an outward relaxation. Note that the numerical error for all calculated inter-layer spacings is about $\pm 0.3\%$ d_0 .

In Fig. 2 we show the Fermi surfaces for the clean Mo(110) surface and for the H-covered surface. On the left the theoretical results of the N -particle ground state are plotted and the right side displays the experimental ARP data of Jeong *et al.* [13]. For the adsorbate system we present the results for the hollow position.

The shaded areas are the projection of the bulk Fermi surface onto the (110) SBZ. For the experimental analysis it was calculated using a tight-binding interpolation scheme [22]. Differences between this projection and the one of the present work may arise from the lack of self-consistency of the tight-binding approach. For the clean surface (see Fig. 2a) the calculations identify four bands, which are highly localized at the surface. There is a band-circuit centered at $\bar{\Gamma}$, one centered at \bar{S} , and one centered at \bar{N} . Furthermore, there is a band more or less parallel to the $\bar{\Gamma}\bar{N}$ direction. The latter one is of $(d_{3z^2-r^2}, d_{xz})$ character, and also the other surface features are due to Mo d bands. All of these bands have been observed experimentally, and for all of them the calculated and measured \mathbf{k} -dependence is in very good agreement (compare Figs. 2a and b). Clearly worse agreement is found when we compare the results for the adsorbate systems (see Fig. 2, lower panels).

At first we discuss the changes of the theoretical Fermi

surface induced by the hydrogen adsorption (Fig. 2a and c), and then we return to the experiments. For the present discussion the most important effect is that the $(d_{3z^2-r^2}, d_{xz})$ band is shifted away from the $\bar{\Gamma}\bar{N}$ line. A significant fraction is now in the stomach shaped band gap. This shift is not a consequence of hybridization between the $(d_{3z^2-r^2}, d_{xz})$ states and hydrogen orbitals but it results because the adsorption of hydrogen changes the surface potential and shifts the entire $(d_{3z^2-r^2}, d_{xz})$ band to lower energies. As this band disperses upward when \mathbf{k} increases away from $\bar{\Gamma}$, the Fermi energy cuts the shifted band at a longer \mathbf{k} -vector. The hydrogen induced bonding states are found at lower energies (about 5 eV below the Fermi level), and the antibonding states are at higher energies (about 4 eV above the Fermi energy).

Figure 2c reveals that the Fermi-surface contours associated to the $(d_{3z^2-r^2}, d_{xz})$ -like band run parallel to the $\bar{\Gamma}\bar{N}$ direction and perpendicular to $\bar{\Gamma}\bar{S}$ in significant parts of the SBZ giving rise to a quasi-one-dimensional nesting. The \mathbf{k} -vectors connecting these bands in different sections of the Brillouin zone are $\mathbf{Q}_{c1}^{\text{th}}$ and $\mathbf{Q}_{c2}^{\text{th}}$. We recall that the highest occupied Kohn-Sham level of the self-consistent N -electron calculation equals the electron chemical potential, i.e. the Fermi level. However, the Kohn-Sham Fermi surface is (in principle) not an observable. The agreement between Fig. 2a and b and the fact that the wave function character does not change significantly upon hydrogen adsorption suggests that the difference between the Kohn-Sham Fermi surface and the true Born-Oppenheimer Fermi surface is not very important for this system. We therefore conclude that the nesting instability predicted by the Fermi surface of Fig. 2c can be trusted, and due to its one-dimensional nature we expect important consequences [23]. Such an instability may induce a static distortion provided that the electronic energy gain is stronger than the elastic energy cost needed to displace the top layer atoms. Because the (110) surface is the closest packed and most stable bcc surface such a Peierls distortion is somewhat unlikely. When a static distortion is not realized, there will be strong dynamical consequences (similar to a dynamical Jahn-Teller effect in molecules) due to thermally excited electron-hole pairs with a wavevector equal to the critical wavevectors and their coupling to surface phonons.

Since for metal surfaces helium atoms scatter at a distance of about 3-4 Å in front of the surface HAS will detect electron charge density oscillations close to the Fermi level [25]. For the system Mo(110) at the critical wave vectors these oscillations are associated with electron-hole pair excitations involving the $(d_{3z^2-r^2}, d_{xz})$ band. We therefore propose that the two bands seen by HAS are due to a hybridization between lattice vibrations and electron-hole pairs. Thus these studies represent an experimental manifestation of a nearly one-dimensional Kohn anomaly. While the small dip is due to a more phonon like excitation, the sharp and giant

anomaly is due to a more electron-hole like excitation of nested electron-hole pairs. The anomalies persist in the phonon dispersion curves along directions deviating from $\overline{\Gamma\text{H}}$ [2,3]. This result is directly understandable in terms of the theoretical results of Fig. 2c, because nesting is present also for the directions in the surface Brillouin zone out of the [001] azimuth. Because of the form of the $(d_{3z^2-r^2}, d_{xz})$ band Fermi-surface contour, the anomalies are particularly strong along $\overline{\Gamma\text{S}}$ in agreement with the available experimental data [3]. We expect a weakening of the indentations for directions between $\overline{\Gamma\text{H}}$ and $\overline{\Gamma\text{S}}$ because of the less effective nesting. A careful reanalysis of the experimental data is in progress [24].

Our interpretation of the HAS results also explains why in HREELS only the Rayleigh mode with the small dip was observed. This technique couples to vibrations of the nuclei and is practically insensitive to electronic charge density oscillations [25]. Because the sharp and giant anomaly has only little vibrational character, it is practically impossible to excite it by high-energy electrons.

The important question remains why the ARP measurements for the hydrogen covered Mo(110) and the theoretical Kohn-Sham Fermi surface are so much different. The results of Fig. 2c are due to photoelectrons which carry the information about the difference of the N particle ground state and the $N - 1$ particle system with a hole at $|\epsilon_F, \mathbf{k}\rangle$. Typically an analysis is done under the assumption that the electronic system is in its ground state and that vibrational excitations as well as interactions between electronic and vibrational excitations can be ignored. The theoretical results shown in Fig. 2c, which are obtained under exactly this hypothesis, disclose that for this system the assumption is unfounded. In fact, the calculations predict highly localized parallel bands at the Fermi surface with a one-dimensional nesting vector. As a consequence, at \mathbf{Q}_{c1} and \mathbf{Q}_{c2} many electron-hole pairs will be thermally excited, and these will couple to phonons. This implies a breakdown of the Born-Oppenheimer approximation. While the calculations identify a strong nesting, the ARP experiments investigate a system which has already reacted to this instability. When a static distortion is hindered, ARP will measure a state with a significant number of low energy excitations, and in particular at the critical wave vectors the electron and lattice dynamics cannot be decoupled. In fact, we note that the experimental Fermi surface of the H covered surface seems to exhibit a different translational symmetry than that of the (1×1) SBZ (see the band circuits at the $\overline{\text{S}}$ point in Fig. 2d). We cannot rule out, however, that this is due to inaccuracies in the experimental data or analysis. We are not aware that for any other surface such a serious breakdown of the Born-Oppenheimer approximation (compare Figs. 2c and d) has been observed so far. Therefore, some doubts remain at this point if an alternative explanation may

exist which can also resolve the differences of the experimental ARP data and the calculated results. Obviously, the static distortion of the W(100) surface is also induced by a Kohn anomaly, but after the reconstruction has taken place the Born-Oppenheimer approximation is again valid.

In conclusion, the calculated Kohn-Sham Fermi surface can explain the HAS and HREELS experiments. It is interesting that the same band which is responsible for the pronounced Kohn anomaly identified above for Mo(110) is in fact also responsible for notable features of all group VIA materials. In particular we mention the spin-density wave in bulk Cr and the phonon anomalies along the [001] direction in bulk W and Mo. Also the reconstruction of Mo(100) and W(100) is induced by the nesting of this band. What makes the anomaly at the (110) so particularly strong is that the adsorption of hydrogen shifts it into a region of \mathbf{k} -space where it becomes localized at the surface. Thus the band becomes two- and the nesting one-dimensional. Neither the hydrogen wave functions nor the hydrogen vibration are *directly* involved in the resulting anomalies. The effect of hydrogen is mainly to change the potential at the surface and to shift the Mo surface states. Thus, it is well possible, that other adsorbates can have a similar effect on the surface vibrations and electron-phonon coupling. We also expect that for the clean surface a weak signature of the $(d_{3z^2-r^2}, d_{xz})$ band should exist at $\mathbf{k} \approx 0.6 \text{ \AA}^{-1}$. However, for the clean surface the band is not a surface state but a broad and less localized surface resonance. The thermal excitations of electron-hole pairs at Mo(110):H and the suggested breakdown of the Born-Oppenheimer approximation call for additional photoemission experiments, in which the Fermi surface is carefully studied also at lower temperatures. In fact, also a detailed analysis of the temperature dependence of the small dip seen in HAS and HREELS would be most interesting. Furthermore, calculations of the electron-phonon coupling, electron-hole excitations and frozen phonons at these surfaces would be very helpful, but for transition metal surfaces this is not yet feasible with the required accuracy.

We thank J. Lüdecke, E. Hulpke, and E. Tosatti for stimulating discussions.

-
- [1] E. Hulpke and J. Lüdecke, Surf. Sci. **272**, 289 (1992); Phys. Rev. Lett. **68**, 2846 (1992).
 - [2] E. Hulpke and J. Lüdecke, Surf. Sci. **287/288**, 837 (1993); J. Electron. Spectr. Relat. Phenom. **64/65**, 641 (1993).
 - [3] J. Lüdecke, Ph.D. thesis, Universität Göttingen(1994).
 - [4] From Ref. 4 it results that the anomalies along $\overline{\Gamma\text{S}}$ occur at the zone boundary and not slightly away from $\overline{\text{S}}$ as

reported in Refs. 2 and 3. An errata of Hulpke and Lüdeke is in preparation.

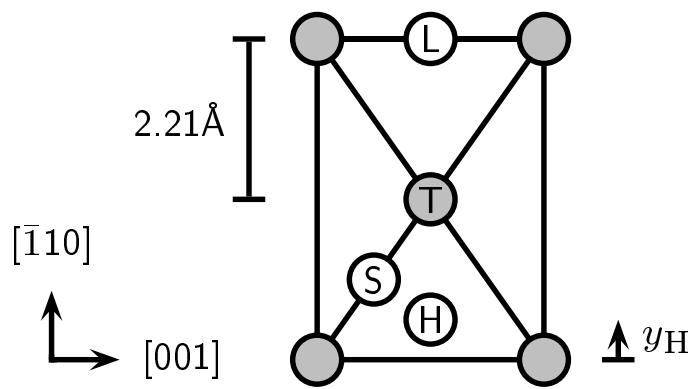
- [5] B. Renker, L. Pintschovius, W. Gläser, H. Rietschel, and R. Comes, in *Lecture Notes in Physics*, Vol. 34 (Springer, Berlin, 1975), p. 53.
- [6] H.-J. Ernst, E. Hulpke, and J. P. Toennies, Phys. Rev. Lett. **58**, 1941 (1987); Europhys. Lett. **10**, 747 (1989); Phys. Rev. B **46**, 16081 (1992).
- [7] E. K. Schweizer and C. T. Rettner, J. Vac. Sci. Technol. A **7**, 1937 (1989).
- [8] E. Hulpke and D.-M. Smilgies, Phys. Rev. B **40**, 1338 (1989).
- [9] K. E. Smith, G. S. Elliott, and S. D. Kevan, Phys. Rev. B **42**, 5385 (1990).
- [10] J. W. Chung *et al.*, Phys. Rev. Lett. **69**, 2228 (1992).
- [11] L. Jupille and D. A. King, in *The Chemical Physics of Solid Surfaces, Vol. 7*, ed. by D. A. King and D. P. Woodruff (Elsevier, Amsterdam, 1994), p. 35.
- [12] K. H. Jeong, R. H. Gaylord, and S. D. Kevan, Phys. Rev. B **38**, 10302 (1988).
- [13] K. H. Jeong, R. H. Gaylord, and S. D. Kevan, Phys. Rev. B **39**, 2973 (1989); J. Vac. Sci. Technol. A **7**(3), 2199 (1989).
- [14] R. H. Gaylord, K. H. Jeong, and S. D. Kevan, Phys. Rev. Lett. **62**, 2036 (1989).
- [15] M. Balden, S. Lehwald, E. Preuss, and H. Ibach, Surf. Sci. **307/309**, 1141 (1994).
- [16] D. M. Ceperley and B. J. Alder, Phys. Rev. Lett. **45**, 566 (1980); J. P. Perdew and A. Zunger, Phys. Rev. B **23**, 5048 (1981).
- [17] P. Blaha, K. Schwarz, P. Sorantin, and S. B. Trickey, Comput. Phys. Commun. **59**, 399 (1990); P. Blaha, K. Schwarz, R. Augustyn, WIEN93, Technische Universität Wien, 1993.
- [18] R. Yu, D. Singh, and H. Krakauer, Phys. Rev. B **43**, 6411 (1991).
- [19] K. W. Katahara, M. H. Manghnani, and E. S. Fisher, J. Phys. F **9**, 773 (1979).
- [20] M. Methfessel, D. Hennig, and M. Scheffler, Phys. Rev. B **46**, 4816 (1992).
- [21] M. Altman, J. W. Chung, P. J. Estrup, J. M. Kosterlitz, J. Prybyla, D. Sahu, and S. C. Ying, J. Vac. Sci. Technol. A **5**, 1045 (1987).
- [22] D. A. Papaconstantopoulos, *Handbook of the Band Structure of Elemental Solids*, Plenum, New York, 1986.
- [23] E. Tosatti, Festkörperprobleme **15**, 113 (1975).
- [24] E. Hulpke, private communication.
- [25] C. Kaden, P. Ruggerone, J. P. Toennies, G. Zhang, and G. Benedek, Phys. Rev. B **46**, 13509 (1992).

FIG. 1. Surface geometry of Mo(110) with the long-bridge (L), short-bridge (S), hollow (H) and on-top (T) sites marked. y_H is the $[\bar{1}10]$ -offset of the hollow position from the long-bridge site.

FIG. 2. Fermi surfaces of clean Mo(110) [upper panels] and Mo(110) with a full monolayer of hydrogen [lower panels]. The experimental results are from [13]. Shaded areas are the projection of the bulk Fermi surfaces onto the (110) surface Brillouin zone. The solid (dotted) lines of the theoretical results denote surface resonances or surface states which are localized by more than 60 % (30 %) in the two top Mo layers. $\mathbf{Q}_{c1}^{\text{th}}$ and $\mathbf{Q}_{c2}^{\text{th}}$ are the theoretical critical wavevectors.

	clean	hollow	long bridge	short bridge	on top
$d_{\text{H-Mo}}$ (Å)	—	1.07	1.08	1.32	1.76
Δd_{12} (% d_0)	-4.5	-2.1	-1.9	-2.8	+1.8
Δd_{23} (% d_0)	+0.5	+0.1	-0.1	+0.3	-1.2
Δd_{34} (% d_0)	0.0	-0.1	-0.3	-0.3	+0.1
ΔE_{ad} (eV)	—	0.0	-0.23	-0.28	-1.11

TABLE I. Calculated geometries and adsorption-energy differences for clean Mo(110) and for the H-covered surface. For the latter the results for the long-bridge, short-bridge, hollow, and on-top sites (see Fig. 1) are compiled. $d_{\text{H-Mo}}$ represents the height of the hydrogen atom above the surface while Δd_{ij} is the percentage change of the inter-layer distance between the i -th and the j -th layer with respect to the bulk inter-layer spacing d_0 .



theory

experiment

